

Brute-forcing spin-glass problems with CUDA

Konrad Jałowiecki^{a,*}, Marek M. Rams^b, Bartłomiej Gardas^{b,a}

^a*Institute of Physics, University of Silesia, Uniwersytecka 4, 40-007 Katowice, Poland*

^b*Jagiellonian University, Marian Smoluchowski Institute of Physics, Łojasiewicza 11, 30-348 Kraków, Poland*

Abstract

We demonstrate how to compute the low energy spectrum for small ($L \leq 50$), but otherwise arbitrary, spin-glass instances using modern Graphics Processing Units or a similar heterogeneous architecture. Our algorithm performs an exhaustive (i.e. brute-force) search of all possible configurations to select $N \ll 2^L$ lowest ones together with their corresponding energies. We mainly focus on the Ising model defined on an arbitrary graph. An open source implementation based on CUDA Fortran and a suitable Python wrapper are provided. As opposed to heuristic approaches ours is exact and thus can serve as a reference point to benchmark other algorithms and hardware, including quantum and digital annealers. Our implementation offers unprecedented speed and efficiency already visible on commodity hardware. At the same time, it can be easily launched on professional, high-end, graphics cards virtually at no extra effort. As a practical application, we employ it to demonstrate that despite its one-dimensional nature, the recent Matrix Product State based algorithm can still accurately approximate the low energy spectrum of fully connected graphs of size L approaching 50.

Keywords: CUDA Fortran, Ising spin-glass, quantum annealers, Titan V GPU

1. Introduction

With increasing complexity and inter-connectivity in the modern world the ability to solve optimization problems becomes indispensable. Notwithstanding, these problems are fundamentally hard to resolve as they often require seeking over *enormous* spaces of possible solutions [1]. A notable example is the famous spin glass problem encoded via the Ising model [2], where the low energy spectrum (the ground state in particular) is sought after. The importance of this system is reflected in the fact that many NP-complete [3] optimization problems (i.e. Karp's 21 problems [4]) can be mapped onto its Hamiltonian [5]. Furthermore, there is growing hardware support for many spin glass based models [6, 7, 8]. These cutting edge technologies when combined with classical neural networks [9] lead to quantum artificial intelligence [10]. A type of an artificial intelligence believed to be powerful enough to simulate many body quantum systems *efficiently*, which is a holy grail of modern physics [11].

The most promising ideas to overcome mathematical difficulties concerning classical optimization could rely on quantum computers [12]. In particular, on quantum annealers such as the D-Wave 2000Q chip [13]. In principle, such machines could solve variate of (hard) optimization problems (almost) “naturally” by finding low energy eigenstates [14]. However, current quantum annealers are extremely noisy and thus not powerful enough to tackle large scale optimization challenges [15, 16]. In contrast, heuristic approaches, often offering superior performance, can *not* typically certify that the solution that has been

found is in fact optimal [17, 18]. Most heuristic solvers rely on strategies ranging from famous simulated annealing [19], branch and bound approaches [20] their chordal extension [18], various Monte Carlo methods [21] throughout dynamical systems simulations [22] to tensor network analysis [23].

In this work we focus on yet another class of solvers, namely those that perform exact brute-force search [24]. The idea is to search the entire Hilbert space exhaustively to find configurations with lowest energies. Such search can be performed either in the probability or energy space [23]. For all classical Hamiltonians, where all their terms commute, this is essentially equivalent to the exact diagonalization. However, in contrast to the quantum case, the eigenvalue problem for classical models can be executed truly in parallel. An efficient implementation nonetheless is *not* trivial.

Although practical applications of such solvers are limited to small problem sizes ($L \leq 50$), they can solve the Ising model that is defined on an arbitrary graph. Moreover, with the exhaustive search one can easily certify the output. All of these features are crucial for testing, benchmarking and validating new methods [25], strategies and paradigms (e.g. memcomputing [22]) for solving classical optimization problems [26].

In this work, we employ our solver to test the applicability of a tensor network ansatz based on the Matrix Product State (MPS) to optimization purposes to a fully connected graph of growing size. For detailed description of this algorithm we refer the reader to see Supplementary Information in Ref. [23]. We have verified that indeed such an ansatz, despite its inherited one-dimensional structure, can still successfully capture the low energy spectrum for tested graphs up to $L = 50$. This indicates that the MPS ansatz should still perform well also for

*Corresponding author.

E-mail address: konrad.jalowiecki@smcebi.edu.pl

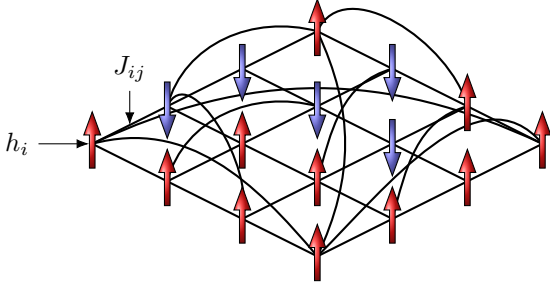


Figure 1: An example of the Ising spin glass model (1). Here, J_{ij} correspond to weights of the edges of the graph and h_i are biases associated with the graph's nodes ($L = 16$). Physically, J_{ij} describe the interaction between spins s_i, s_j and h_i is the external magnetic field imposed on spin s_i . The picture also demonstrate possible spin encoding, with red arrows indicating assignment of $s_i = +1$ and blue ones indicating assignment of $s_i = -1$ [or $s_i = 0$ if QUBO (2) is used].

much larger systems having a dominant quasi-one-dimensional nature. At the same time sparse connections at long range do *not* necessary exclude applicability of the MPS approach.

Our implementation offers great flexibility and portability as well as the necessary efficiency and speed. Our solver can be executed on either CPU (Central Processing Unit) or GPU (Graphic Processing Unit) using Nvidia's CUDA (Compute Unified Device Architecture). The latter architecture is of particular importance due to its massive parallel capabilities [27, 28]. We provide a simple Python wrapper that allows users to access both architectures effortlessly [29].

2. Spin-glass problems

In this work we mainly focus on the Ising Hamiltonian. However, our approach can easily be extended to include other *classical* spin-glass models [30, 31]. To begin with, consider a simple undirected graph with L nodes (i.e. vertices) as the one drawn in Fig. 1. We assign a unique spin variable, $s_i \pm 1$ (blue and red arrows), to each node. Adjacent nodes labeled as i, j are coupled via interaction strength J_{ij} , which may be viewed as a weight of the edge connecting those two nodes. Additionally, for every spin we associate a local magnetic field (bias) h_i interacting with it. Then the energy of such a system of spins is defined as

$$H(s) = - \sum_{\langle i,j \rangle} J_{ij} s_i s_j - \sum_{i=1}^L h_i s_i, \quad (1)$$

where $s := (s_1, \dots, s_L)$. The first sum runs over all adjacent sites, which we denote here as $\langle i, j \rangle$.

In many practical applications, one is typically interested in finding a particular spin configuration, say s_0 , for which $H(s_0)$ in Eq. (1) admits its minimum value. Such configuration is called the *ground state*. Naturally, states with energies above the ground state energy are called *excited states*. Finding the low energy spectrum (consisting of the ground state energy and a number $N \ll 2^L$ of excited states) of the Ising model (1) can also be formulated as a Quadratic Unconstrained Optimization

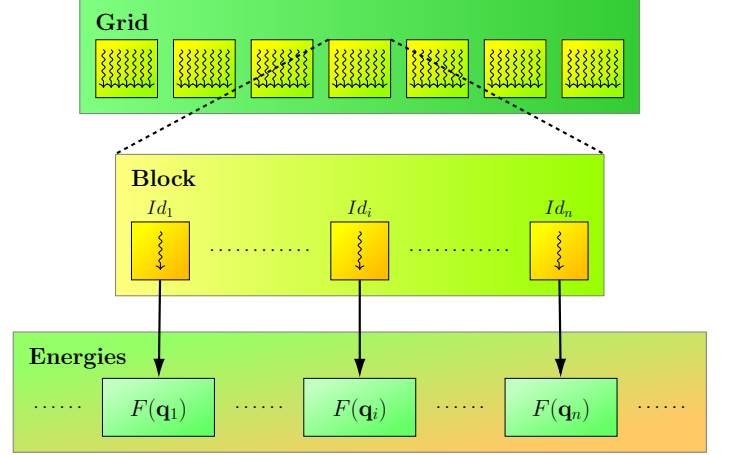


Figure 2: Scheduling of the energy computation on the GPU. A CUDA program is executed by threads that are organized by blocks. Both the grid and blocks can form one, two or three dimensional structures. Our implementation uses a one dimensional grid structure, where the global thread index, Id_i , is converted into a state q with mapping $Id_i = (q)_2$, cf. Eq. (4). Next, each thread in each block computes its own energy, $F(q)$, according to Eq. (3). To fit into, often limited, GPU memory the computation is executed in carefully tailored chunks.

Problem (QUBO). Namely,

$$F(q) = - \sum_{\langle i,j \rangle} a_{ij} q_i q_j - \sum_{i=1}^L b_i q_i, \quad (2)$$

where $q = (s + 1)/2$ are *binary* variables whereas

$$a_{ij} = 4J_{ij}, \quad b_i = 2h_i - 2 \sum_{\langle i,j \rangle} J_{ij}. \quad (3)$$

Note, if a given q_i vanishes so does any product $q_i q_j$. Therefore, QUBO formulation (2) *effectively* reduces the number of multiplications almost by half in comparison to Eq. (1).

Despite its very simple formulation, the problem of solving spin glass instances can *not* be easily tackled using a brute force approach even for a modest number of spin variables. This is since the number of possible spin assignments grows exponentially with the number of nodes in the graph. For instance, when $L = 40$ the number of possible states is greater than the number of bits in a 32GB memory chip. Already when $L = 64$, size of the search space is greater than the estimated age of the Universe in seconds [32]. In fact the problem of finding the ground state of the Ising model defined on an arbitrary graph is long known to be NP-hard [33]. This means, in particular, that even verifying if a given configuration minimizes the cost function (1) is difficult.

3. Description of the algorithm

A general idea underlying this work is to perform an exhaustive search over the whole state space, taking advantage of massive parallel capabilities of modern GPUs. This requires an efficient strategy to encoding all states, $q = (q_1, q_2, \dots, q_L)$, on a GPU. A naive approach would required storing an array of L integers, $q_i = 0, 1$, for each state q . However, this would also

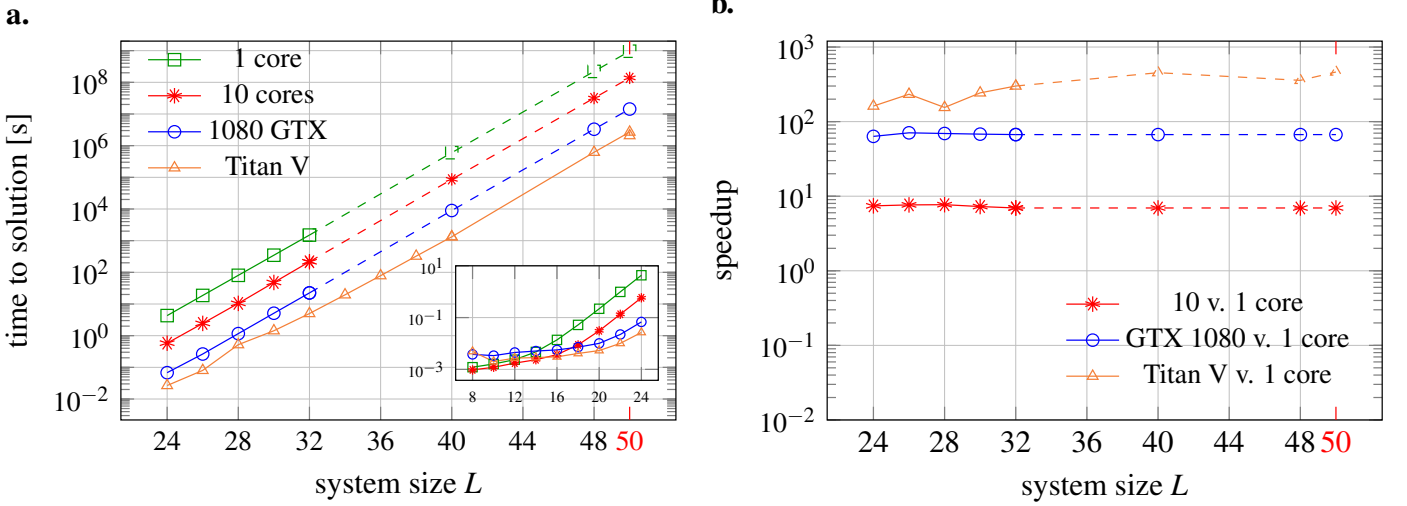


Figure 3: **a.** Time to solution obtained by our solver for various system sizes L . **b.** Calculated speedup in comparison to a single CPU core. The speedup is obtained as a ratio of respective execution times. The algorithm computes $N \ll 2^L$ low energy states in a single run (here $N = 10^2$). The problem instances (J_{ij}, h_i) , on a fully connected graph, were randomly generated. The solid lines show actual measurements: 100 repetitions for each L except for $L = 48$ and $L = 50$ for which time to solution was calculated only once. The dashed lines represent *experimentally* estimated values for larger system sizes. The estimate is based on the time necessary to process a single chunk of data [of size of size $M = 2^{29}$ (CPU), $M = 2^{28}$ (Titan V) and $M = 2^{27}$ (GTX 1080)]. For $L \geq 24$ the overhead of parallel computations starts playing less important role and the execution time becomes linear in the state space size.

lead to an excessive use of memory and render this approach inefficient. As an optimal strategy, one should try to reuse information already stored in the GPU memory. Therefore, in our algorithm we take advantage of the following correspondence

$$\text{GPU thread index} = (q)_2, \quad (4)$$

where $k = (q)_2$ denotes the binary representation of an integer k . For instance, when there is $L = 8$ spins, one may associate

$$\text{thread index \#13} = (00001101)_2, \quad (5)$$

Theoretically, this strategy allows one to store $M = 2^{64} \sim 10^{19}$ states with no extra cost, limiting the system size to $L = 64$ spins. This is, nonetheless, more than the current architecture based on the von Neumann paradigm of computation can process in a reasonable time [34]. Indeed, we estimated that optimal search among 2^{64} states to extract the low energy spectrum consisting of $N = 10^2$ of them would take 821 years on an efficient Titan V GPU [35]. In comparison, systems of sizes $L = 32, 49, 50$ can be solved within 5 seconds, 12 and 24 days, respectively. A detailed benchmark is presented in Sec. 5.

In theory, one could first compute all $M = 2^L$ energies in parallel and only then select $N \ll 2^L$ lowest ones (and the corresponding states if needed). However, even with an efficient storage strategy this approach quickly becomes impractical for large systems. It requires an exponentially increasing storage space to encode possible solutions. To overcome this problem one could iterate over the solution space in manageable chunks, each time extracting the desired number of states (e.g. with the bucket select algorithm [36]). Sorting the energies is executed only in the final step. Since GPU threads and blocks are labelled in the same way for every chunk, an offset, $m = 2^{L-k} - 1$, is

added to the thread index to correctly enumerate all states, i.e.,

$$\text{GPU thread index} + m = (q)_2, \quad (6)$$

Note, the energy calculations are independent and thus can be performed in parallel. It is needless to say that the overall parallel speedup is limited by the serial part (Amdahl's law [37]) consisting of the lowest energy states extraction and merging all local information into the global record. Algorithm 1 in the below listing summarizes the underlying structure of our solver.

4. Implementation details

4.1. Languages and technologies employed

The core components of our implementation has been written in modern Fortran 95/2003 [38], which we have chosen for its flexibility [39], extensive support for linear algebra [40], performance [41] and native support for CUDA technology [42]. To make our code easier to use we have wrapped it in a Python package using the f2py [43] utility and numpy's fork of distutils package [44]. Whereas Fortran is widely used mostly for numerical simulations [45], Python is one of the most popular general purpose programming language [46].

We have also incorporated the Thrust library [47] into our solver for its parallel implementation of many standard methods such as finding the minimum and maximum of an array or partitioning thereof. The Thrust library is utilized both for the GPU implementation as well as for the pure CPU implementation with the OMP backed. In order to take advantage of various Thrust's functions we have written several small C++ modules to bind them into the Fortran code. The source code of the entire

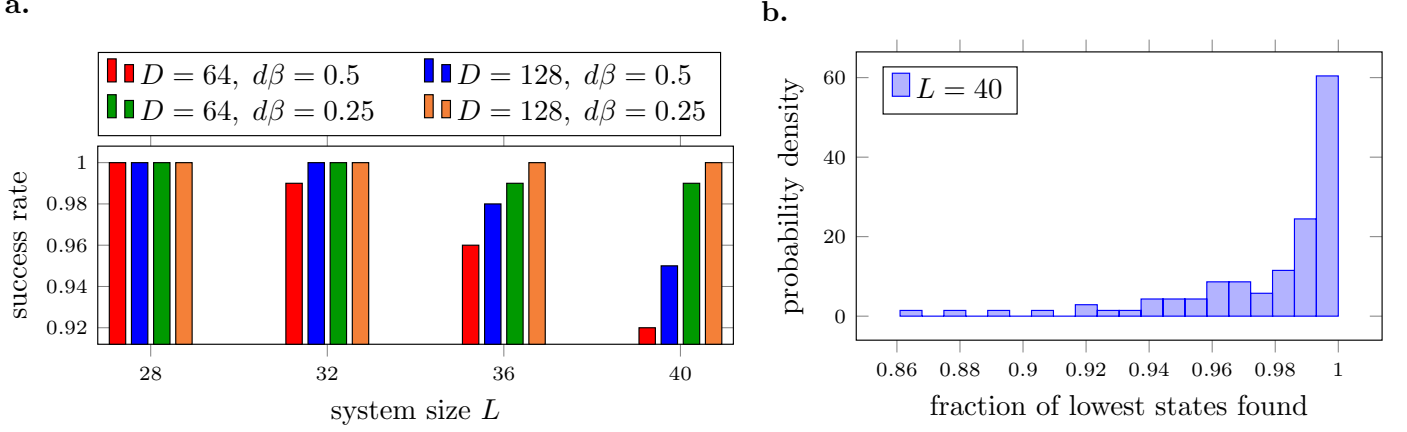


Figure 4: Verification of the Matrix Product State (MPS) based algorithm introduced in Ref. [23]. **a.** Success rate is defined as the fraction of cases for which the MPS algorithm was able to find the ground state. All spin-glass instances were generated randomly on a fully connected graph of size L . Parameter D is the bond dimensions characterizing MPS tensors and $d\beta$ denotes the increment of the inverse temperature, see the main text. **b.** Normalized histogram showing the percent of instances for which the MPS based algorithm was able to find a given number of configurations out of $N = 1000$ lowest ones. Here, we use $D = 128$, $d\beta = 0.25$ and in all panels $\beta = 1$.

Algorithm 1 Searching $N \ll 2^L$ configurations (i.e. states) with the lowest energies defined in Eq. (1). The adjacency matrix, J_{ij} , and local magnetic fields, h_i , are provided.

```

k ← chunk_size
for i = 1 to  $2^{L-k}$  do
  for j = 1 to  $2^k$  do
    state_code ←  $j + (i - 1) \cdot 2^k$ 
    energies[j] ← energy(graph, state_code)
    states[j] ← state_code
  end for
  select_lowest(energies, states, num_st)
  if i == 1 then
    low_en[1 : num_st] ← energies[1 : num_st]
    low_st[1 : num_st] ← states[1 : num_st]
  else
    low_en[num_st + 1 : 2 · num_st] ← energies[1 : num_st]
    low_st[num_st + 1 : 2 · num_st] ← states[1 : num_st]
    select_lowest(low_en, low_st, num_st)
  end if
end for
sort_by_key(low_en, low_st, num_st)

```

package together with the comprehensive documentation can be found on GitHub [29].

The Python wrapper allows one to execute the algorithm both on the CPU and GPU. It was designed with simplicity in mind and as such its basic usage does *not* require any special knowledge. Basic understanding of the underlying physics is enough. In particular, only the system definition (i.e. the graph or adjacency matrix) and the desired number of states needs to be provided by the user. Nevertheless, other parameters including the chunks size can also be passed to the wrapper. The below listing demonstrates its very basic usage.

Listing 1: Simple example of how to use the `ising` module

```

# import package
from ising import search

# adjacency matrix (problem definition)
graph = {(1,1):-1, (1,2):-0.2}
# solve the Ising model
solution = search(graph, num_states=4)

# shows the states and energies found
print(solution.energies)
print(list(solution.states))

```

On virtually all Linux platforms, it is possible to install the very basic version (i.e. with no GPU support) of our solver directly from the Python Package Index, by issuing

$$\text{pip install ising} \quad (7)$$

where `ising` is the name of our package. However, to assure full compatibility with modern GPUs, CUDA support requires a custom build from source which can be initiated via

$$\text{python install.py --usecuda} \quad (8)$$

from the package source directory. For more details regarding custom installation, including CUDA and three major Fortran compilers, we refer the reader to documentation [48].

4.2. GPU execution scheduling

Programming GPUs often pose a nontrivial endeavor. Among many things, one has to design the grid on which kernels are launched [49]. We have tested various grid/blocks launching configurations for our energy computing kernel and have obtained the best results with grids consisting of $G = 2^{g-5}$ (g being the current chunk size) blocks of size $B = 2^5$ each. Note, this particular configuration may need further adjustment depending on the hardware and problem size.

4.3. Complexity analysis

Our algorithm performs an exhaustive search over the entire, exponentially large, state space in predefined chunks to find N lowest states (cf. Algorithm 1). Thus, unavoidably its time complexity has to be at least exponential in the system size L . Computing the energy (2) for a single state, q , requires $O(L^2)$ operations. The selection procedure executed on a data chunk of size 2^k , however, requires $O(2^k)$ comparisons resulting in $O[2^k(L^2 + 1)]$ operations. Finally, taking into account the total number of chunks, 2^{L-k} , and adding complexity of the final sorting procedure, $O[N \log(N)]$, results in total complexity being

$$O[2^L(L^2 + 1) + N \log(N)] = O[2^L(L^2 + 1)]. \quad (9)$$

Therefore, essentially the solver's complexity behaves as $O(2^L)$ which we also demonstrate experimentally in Sec. 5 (cf. Fig. 3).

As one can see, the GPU implementation takes 30 seconds (GeForce 1080) and 5 seconds (Titan V) on average to solve the Ising problems with $L = 32$ spins. The same problems requires about 1500 seconds on average on a single CPU core. For GPU the differences in solution times between single and double precision are close to 10% and are not reported on Fig. 3.

5. Benchmarks

5.1. GPU vs CPU comparison

We have tested our algorithm on the following hardware:

- CPU: 10 Cores Intel^R CoreTM i7-6950X;
- GPU(1): Nvidia GeForce GTX 1080, 8GB GDDR5 global memory, 2560 CUDA Cores;
- GPU(2): Nvidia Titan V, 12GB GDDR5 global memory, 5120 CUDA Cores.

For benchmarking purposes we have executed our algorithm on a fully connected, $K = 100$ randomly generated (cf. Ref. [50, 51]), problem instances for systems sizes of $L = 24, 32$. For each instance, we have calculated the low energy spectrum consisting of $N = 10^2$ states in a single run. Typical results obtained with a high-end CPU (i7-6950X) and both a mid-class (GeForce 1080) and professional (Titan V) GPU are depicted in Fig. 3. We

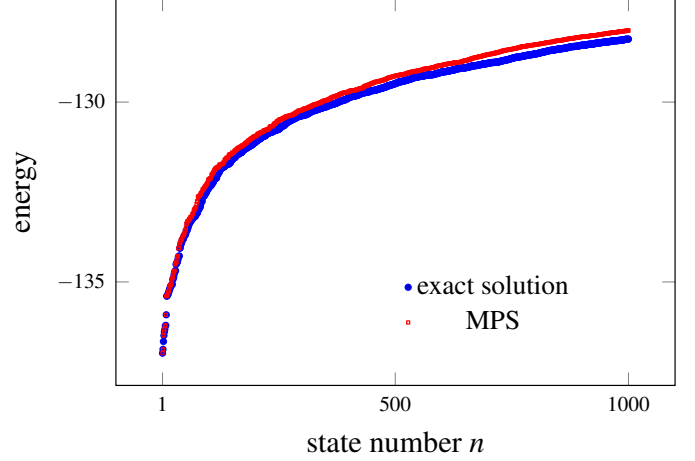


Figure 5: Low energy spectrum of the Ising model (1) obtained with two different algorithms and randomly generated instances of size $L = 50$. Here, the bond dimension for the MPS based algorithm $D = 128$ and the increment of the inverse temperature $d\beta = 0.25$ (cf. the main text or Ref. [23] for more details).

have also *experimentally* estimated time to solution for larger systems (up to $L = 50$ spins) for which the low energy spectrum can be obtained in a reasonable time (i.e. one month). The estimate is based on the average time required to process a single chunk of data [of size $M = 2^{29}$ (CPU), $M = 2^{28}$ (Titan V) and $M = 2^{27}$ (GTX 1080)]. Our measurements are consistent with the complexity analysis discussed in Sec. 4.3.

5.2. Validation of MPS algorithm

To demonstrate capabilities of our solver we use it to benchmark a more sophisticated, *heuristic*, approach based on Matrix Product States (MPS) technique [23]. Here, we are not interested in time to solution but rather we would like to investigate the accuracy of the latter. Heuristic algorithms can often solve large systems ($L \gg 50$), however they cannot certify solutions.

With the MPS based algorithm one aims at approximating the Boltzmann distribution $e^{-\beta H(s)/2} \approx A^{s_1} A^{s_2} \dots A^{s_L} = |\Psi(s)\rangle$ for sufficiently large inverse temperature β , where each A^{s_i} ($i = 1, 2, \dots, L$) is a matrix of size $\leq D$. The bond dimension D reflects on the amount of entanglement which can be “stored” in a quantum system [52] – here understood as superposition over all possible classical spin configurations. The state $|\Psi(s)\rangle$ is obtained by starting with $\beta = 0$, for which the MPS decomposition is trivial, and subsequently applying gates simulating the action of $e^{-d\beta s_i(\sum_{(i,j)} J_{ij} s_j + h_i)}$. Application of those gates results in – in principle exponential – growth of the bond dimension. The one-dimensional loop-less structure of the MPS ansatz allows one, however, to systematically find its approximation which maintains the bond dimension limited to D . Having $|\Psi(s)\rangle$ in the form of MPS, we can then calculate any marginal probability described by $|\Psi(s)\rangle$ and systematically search for most probable classical configurations i.e. the ones with the smallest energies [23].

The question then becomes how well the MPS ansatz, by construction being one-dimensional, is able to encode the structure

of low energy spectrum for fully-connected graphs. In general, the bigger the system the higher D necessary to faithfully capture the structure of low energy spectrum. We observe that already moderate D of 128 is enough to find all ground states for $K = 100$ considered instances, see Fig. 4a. It is also enough to recover most of the 1000 configurations with lowest energies for those instances, see Fig. 4b for $L = 40$. A typical low energy spectrum consisting of $N = 10^3$ states is shown in Fig. 5 for $L = 50$. While all applied gates formally commute, due to the finite numerical precision and finite D , it is relevant to reach the final inverse temperature, β , gradually in a couple of consecutive steps, each with smaller $d\beta$, see Fig. 4a.

6. Summary

We have demonstrated how to perform an exhaustive (brute-force) search in the solution space of the Ising spin-glass model [2] utilizing modern Graphics Processing Units [53]. Moreover, our algorithm can also be adapted for different heterogeneous architectures (e.g. Xeon Phi [54]). The Hamiltonian of this particular model encodes variety of important optimization problems [5]. Moreover, this model has also been realized experimentally as a commercially available D-Wave quantum annealer [8].

Our implementation with CUDA Fortran [42] offers unprecedented speed and efficiency already visible on commodity hardware (e.g. GeForce 1080). Furthermore, it can be easily tuned for professional GPUs such as Titan V [35] virtually at no extra effort. To give an example, our algorithm when tailored for the latter GPU can extract the low energy spectrum (consisting of $N = 10^3$ states) in roughly 5 seconds for the spin system admitting $M = 2^{32} \sim 10^9$ different configurations. In comparison, a single CPU core takes on average 25 minutes to finish the same task (cf. Sec. 5 for detailed benchmark).

Admittedly, practical applications of brute-force algorithms are constrained to small problem sizes ($L \leq 50$). However, they can not only solve the spin-glass problems for arbitrary topologies and instances but also certify solutions [24, 17, 18]. These two features are crucial for developing and validating new methods and strategies for solving classical optimization problems [26]. We have explicitly exemplified this point by comparing our algorithm to a sophisticated recent Ising solver based on tensor network techniques [23]. In particular, we have demonstrated that despite its one-dimensional nature, the Matrix Product State ansatz is still able to approximate well the relevant part of the Boltzmann distribution for fully connected graph of $L \leq 50$. Therefore, this suggests that the MPS algorithm should be superior for all problems having a dominant quasi-one-dimensional nature that allow for sparse connections to span the full problem (e.g. chimera graph [55]).

Finally, to benefit the community, we have made our code publicly available as an open source project [29]. Moreover, for those users who lack technical knowledge of Fortran or CUDA we have provided an easy to install and use Python wrapper [29].

Acknowledgments

We appreciate fruitful discussions with Andrzej Ptok, Jerzy Dajka and Piotr Gawron and Masoud Mohseni. We thank Paweł Wasiak for his valuable remarks regarding solver's documentation. We gratefully acknowledge the support of NVIDIA Corporation with the donation of the Titan V GPU used for this research. This work was supported by National Science Center (NCN), Poland under projects 2016/20/S/ST2/00152 (BG) and NCN together with European Union through QuantERA ERA NET program 2017/25/Z/ST2/03028 (MMR). MMR acknowledges receiving Google Faculty Research Award 2017.

References

- [1] Aaronson, S. *Quantum Computing Since Democritus* (Cambridge University Press, 2013).
- [2] Harris, R., et al. Phase transitions in a programmable quantum spin glass simulator. *Science* **361**, 162 (2018) 30002250 .
- [3] Garey, M. R. & Johnson, D. S. *Computers and Intractability: A Guide to the Theory of NP-Completeness* (W. H. Freeman & Co., 1979).
- [4] Karp, R. Reducibility among combinatorial problems. in *Complexity of Computer Computations* (Plenum Press, 1972) pp. 85–103.
- [5] Lucas, A. Ising formulations of many NP problems. *Front. Phys.* **2**, 5 (2014).
- [6] Yamamoto, Y., et al. Coherent Ising machines—optical neural networks operating at the quantum limit. *npj Quantum Inf.* **3**, 49 (2017).
- [7] Aramon, M., et al. Physics-Inspired Optimization for Quadratic Unconstrained Problems Using a Digital Annealer. Preprint at [arXiv:1806.08815](https://arxiv.org/abs/1806.08815) (2018).
- [8] King, J., et al. Benchmarking a quantum annealing processor with the time-to-target metrics. Preprint at [arXiv:1508.05087](https://arxiv.org/abs/1508.05087) (2015).
- [9] Krizhevsky, A., Sutskever, I. & Hinton, G. E. ImageNet Classification with Deep Convolutional Neural Networks. in *Proceedings of the 25th International Conference on Neural Information Processing Systems - Volume 1 NIPS'12* (Curran Associates Inc., 2012) pp. 1097–1105.
- [10] Gardas, B., Rams, M. M. & Dziarmaga, J. Quantum neural networks to simulate many-body quantum systems. *Phys. Rev. B* **98**, 184304 (2018).
- [11] Elsayed, T. A., Mølmer, K. & Madsen, L. B. Entangled Quantum Dynamics of Many-Body Systems using Bohmian Trajectories. *Sci. Rep.* **8**, 12704 (2018).
- [12] Feynman, R. P. There's plenty of room at the bottom. *Caltech Eng. Sci.* **23**, 22 (1960).
- [13] Lanting, T., et al. Entanglement in a quantum annealing processor. *Phys. Rev. X* **4**, 021041 (2014).
- [14] Orus, R. A practical introduction to tensor networks: Matrix product states and projected entangled pair states. *Ann. Phys.* **349**, 117 (2014).
- [15] Gardas, B. & Deffner, S. Quantum fluctuation theorem for error diagnostics in quantum annealers. *Sci. Rep.* **8**, 17191 (2018).
- [16] Gardas, B., Dziarmaga, J., Zurek, W. H. & Zwolak, M. Defects in quantum computers. *Sci. Rep.* **8**, 4539 (2018).
- [17] Jakub Czartowski, B. G. Y. F. K. Ż., Konrad Szymański Ground state energy: Can it really be reached with quantum annealers?. Preprint at [arXiv:1812.09251](https://arxiv.org/abs/1812.09251) (2018).
- [18] Baccari, F., Gogolin, C., Wittek, P. & Acín, A. Verification of quantum optimizers. Preprint at [arXiv:1808.01275](https://arxiv.org/abs/1808.01275) (2018).
- [19] Cook, C., Zhao, H., Sato, T., Hiromoto, M. & Tan, S. X.-D. GPU Based Parallel Ising Computing for Combinatorial Optimization Problems in VLSI Physical Design. (2018) [arXiv:1807.10750](https://arxiv.org/abs/1807.10750) .
- [20] Rendl, F., Rinaldi, G. & Wiegale, A. Solving Max-Cut to optimality by intersecting semidefinite and polyhedral relaxations. *Math. Program.* **121**, 307 (2008).
- [21] Hen, I. Solving spin glasses with optimized trees of clustered spins. *Phys. Rev. E* **96**, 022105 (2017).
- [22] Sheldon, F., Traversa, F. L. & Ventra, M. D. Taming a non-convex landscape with dynamical long-range order: memcomputing the Ising spin-glass. Preprint at [arXiv:1810.03712](https://arxiv.org/abs/1810.03712) (2018).

- [23] Rams, M. M., Mohseni, M. & Gardas, B. Heuristic optimization and sampling with tensor networks for quasi-2D spin glass problems. Preprint at [arXiv:1811.06518](https://arxiv.org/abs/1811.06518) (2018).
- [24] Heule, M. J. H. & Kullmann, O. The Science of Brute Force. *Commun. ACM* **60**, 70 (2017).
- [25] Leleu, T., Yamamoto, Y., McMahon, P. L. & Aihara, K. Destabilization of local minima in analog spin systems by correction of amplitude heterogeneity. *Phys. Rev. Lett.* **122**, 040607 (2019).
- [26] Mandra, S. & Katzgraber, H. G. A deceptive step towards quantum speedup detection. *Quantum. Sci. Technol.* **3**, 04LT01 (2018).
- [27] Januszewski, M., Ptak, A., Crivelli, D. & Gardas, B. GPU-based acceleration of free energy calculations in solid state physics. *Comput. Phys. Commun* **192**, 220 (2015).
- [28] Gardas, B. & Ptak, A. Counting defects in quantum computers with graphics processing units. *J. Comput. Phys.* **366**, 320 (2018).
- [29] Ising (Python package). <https://github.com/dexter2206/ising> (2019) accessed: 2019-01-27.
- [30] Wu, F. Y. The Potts model. *Rev. Mod. Phys.* **54**, 235 (1982).
- [31] Liu, Z., Rodrigues, S. P. & Cai, W. Simulating the Ising model with a deep convolutional generative adversarial network. Preprint at [arXiv:1710.04987v1](https://arxiv.org/abs/1710.04987v1) (2018).
- [32] Ade, P. A. R., et al. Planck 2015 results - XIII. Cosmological parameters. *Astron. Astrophys.* **594**, A13 (2016).
- [33] Barahona, F. On the computational complexity of Ising spin glass models. *J. Phys. A: Math. Gen.* **15**, 3241 (1982).
- [34] Backus, J. Can programming be liberated from the von neumann style?: A functional style and its algebra of programs. *Commun. ACM* **21**, 613 (1978).
- [35] Nvidia Titan V. <https://www.nvidia.com/en-gb/titan/titan-v/> (2018) accessed: 2019-01-27.
- [36] Alabi, T., et al. Fast K-selection Algorithms for Graphics Processing Units. *J. Exp. Algorithmics* **17**, 4.2:4.1 (2012).
- [37] Hill, M. D. & Marty, M. R. Amdahl's Law in the Multicore Era. *Computer* **41**, 33 (2008).
- [38] Chapman, S. J. *Fortran 95/2003 for Scientists & Engineers* (McGraw-Hill, 2007).
- [39] Rossi, L., Berzosa-Molina, J. & Stam, D. M. PYMIEDAP: A Python–Fortran tool for computing fluxes and polarization signals of (exo)planets. *Astron. Astrophys.* **616**, A147 (2018).
- [40] Wang, E., et al. Intel Math Kernel Library. in *High-Performance Computing on the Intel® Xeon Phi™* (Springer, 2014) pp. 167–188.
- [41] Julia Micro-Benchmarks. <https://julialang.org/benchmarks/> (2019) accessed: 2019-01-27.
- [42] Fatica, M. & Ruetsch, G. *CUDA Fortran for Scientists and Engineers* (Elsevier, 2014).
- [43] F2PY Users Guide and Reference Manual — NumPy v1.15 Manual. <https://docs.scipy.org/doc/numpy-1.15.0/f2py/index.html> (2018).
- [44] Packaging (numpy.distutils) — NumPy v1.15 Manual. <https://docs.scipy.org/doc/numpy-1.15.0/reference/distutils.html> (2018) accessed: 2018-10-23.
- [45] Wall, M. L. & Carr, L. D. Out of equilibrium dynamics with matrix product states. *New J. Phys.* **14**, 125015 (2012).
- [46] Stack Overflow Developer Survey 2018. <https://insights.stackoverflow.com/survey/2018/> (2018) accessed: 2019-01-27.
- [47] Thrust - Parallel Algorithms Library. <https://thrust.github.io/> (2015) accessed: 2019-01-27.
- [48] Ising package documentation. <https://ising.readthedocs.io/en/latest/> (2019) accessed: 2019-01-27.
- [49] Sanders, J. & Kandrot, E. *CUDA by Example: An Introduction to General-Purpose GPU Programming* 1st ed. (Addison-Wesley Professional, 2010).
- [50] Marshall, J., Martin-Mayor, V. & Hen, I. Practical engineering of hard spin-glass instances. *Phys. Rev. A* **94**, 012320 (2016).
- [51] Hamze, F., et al. From near to eternity: Spin-glass planting, tiling puzzles, and constraint-satisfaction problems. *Phys. Rev. E* **97**, 043303 (2018).
- [52] Jaschke, D., Wall, M. L. & Carr, L. D. Open source matrix product states: Opening ways to simulate entangled many-body quantum systems in one dimension. *Comput. Phys. Commun.* **225**, 59 (2018).
- [53] Pharr, M. & Fernando, R. *GPU Gems 2: Programming Techniques for High-Performance Graphics and General-Purpose Computation* 1st ed. (Addison-Wesley Professional, 2005).
- [54] Surmin, I. A., et al. Particle-in-Cell laser-plasma simulation on Xeon Phi coprocessors. *Comput. Phys. Commun.* **202**, 204 (2016).
- [55] Choi, V. Minor-embedding in adiabatic quantum computation: I. the parameter setting problem. *Quantum Inf. Process.* **7**, 193 (2008).